

Improved PeT Molecules for Optically Sensing Voltage in Neurons

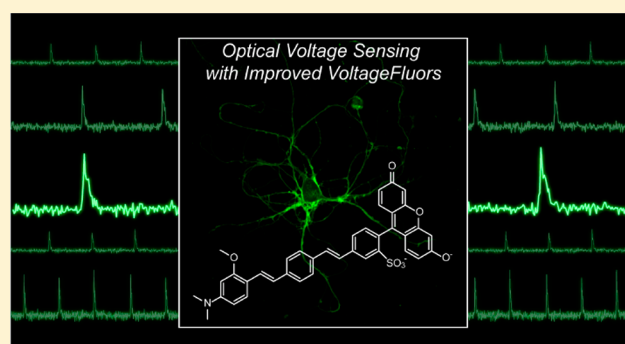
Clifford R. Woodford,^{†,◆} E. Paxon Frady,[§] Richard S. Smith,[○] Benjamin Morey,[‡] Gabriele Canzi,[†] Sakina F. Palida,[⊥] Ricardo C. Araneda,[○] William B. Kristan, Jr.,^{||} Clifford P. Kubiak,[†] Evan W. Miller,^{*,‡,▽,◆} and Roger Y. Tsien^{*,†,‡,#}

[†]Departments of Chemistry and Biochemistry, [‡]Pharmacology, [§]Neurosciences Graduate Group, ^{||}Division of Biological Sciences, [⊥]Biomedical Sciences, and [#]Howard Hughes Medical Institute, University of California, San Diego, La Jolla, California 92093, United States

[○]Department of Biology, University of Maryland, College Park, Maryland 20742, United States

Supporting Information

ABSTRACT: VoltageFluor (VF) dyes have the potential to measure voltage optically in excitable membranes with a combination of high spatial and temporal resolution essential to better characterize the voltage dynamics of large groups of excitable cells. VF dyes sense voltage with high speed and sensitivity using photoinduced electron transfer (PeT) through a conjugated molecular wire. We show that tuning the driving force for PeT ($\Delta G_{\text{PeT}} + w$) through systematic chemical substitution modulates voltage sensitivity, estimate ($\Delta G_{\text{PeT}} + w$) values from experimentally measured redox potentials, and validate the voltage sensitivities in patch-clamped HEK cells for 10 new VF dyes. VF2.1(OMe).H, with a 48% $\Delta F/F$ per 100 mV, shows approximately 2-fold improvement over previous dyes in HEK cells, dissociated rat cortical neurons, and medicinal leech ganglia. Additionally, VF2.1(OMe).H faithfully reports pharmacological effects and circuit activity in mouse olfactory bulb slices, thus opening a wide range of previously inaccessible applications for voltage-sensitive dyes.



INTRODUCTION

The ability to interrogate the dynamics of cellular events with precise spatial and temporal resolution is limited, to a large degree, by the development of fluorescent indicators with sufficient sensitivity and selectivity for events of interest. Changes in electric potential across biological membranes are cellular events of key interest in a number of biological systems such as the heart, muscle, and brain. Understanding the spatial and temporal dynamics of electrical changes in neural activity that underlie basic human behaviors, emotions, perceptions, and thought remains a key challenge to neurobiology. Monitoring transmembrane potential of excitable cells forms the basis for modern neurobiology, yet methods to do so have been limited primarily to electrophysiological recordings with electrodes.¹ This places sharp constraints on the spatial information gleaned from this approach. In general, the size of electrodes and pipettes used for traditional electrophysiology restricts their usage to a single neuronal soma, making recording from either multiple cells simultaneously or from subcellular regions, such as dendritic spines and axonal terminals, extremely difficult or impossible.¹ In a complementary fashion, imaging Ca^{2+} ions has taken center stage for measuring neuronal activity, where the transient increase in $[\text{Ca}^{2+}]_i$ acts as an indirect readout of neuronal activity. However, although Ca^{2+} indicators are highly sensitive and

can, in some cases, be genetically encoded, they provide very little information regarding hyperpolarization, subthreshold events, or the nature of the electrical changes that generated the Ca^{2+} increase.

Imaging voltage dynamics offers an attractive solution to this problem, and several types of voltage-sensitive indicators have been described. These include small molecule fluorescent approaches such as merocyanines,² oxonols, and rhodamines,³ charge-shift electrochromic dyes,^{4–6} lipophilic anions,^{7–10} second-harmonic generation,^{11,12} and nanoparticles.^{13,14} Genetically encoded voltage indicators are also known and make use of fluorescent protein fusions to endogenous voltage-sensing domains^{15–20} or microbial opsins^{21,22} to transduce voltage changes into photons. Limitations of these and other voltage-sensitive indicators include combinations of low sensitivity, slow response kinetics, high capacitive load, low brightness, and poor membrane localization.

In an effort to help meet the need for indicators that faithfully report on voltage changes with high spatial and temporal resolution, we recently disclosed the initial design and characterization of VoltageFluor 2.1.Cl (VF2.1.Cl) for imaging voltage changes in neurons with high spatial and temporal

Received: October 15, 2014

Published: January 13, 2015

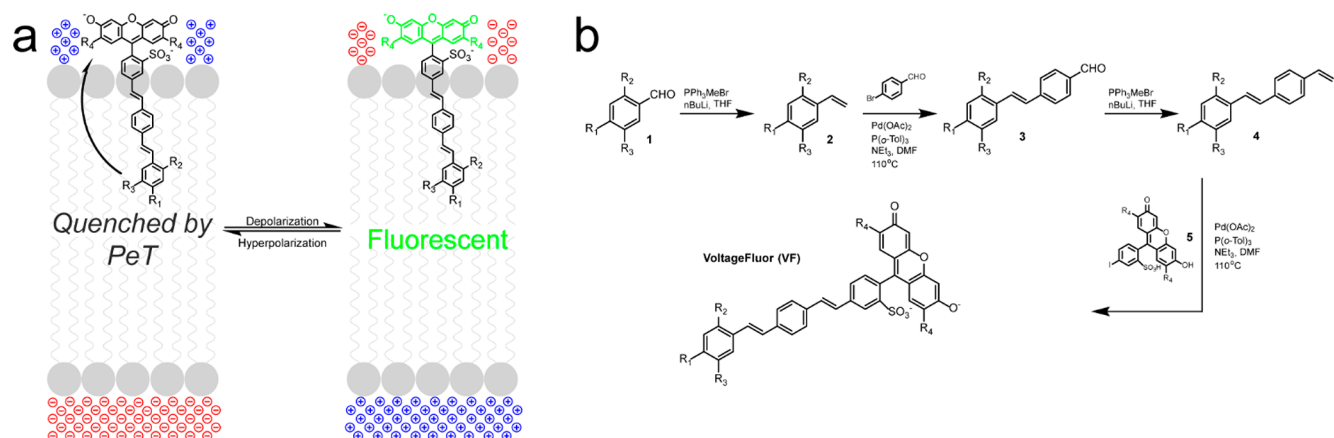


Figure 1. Voltage-sensing mechanism and synthesis of VoltageFluor dyes. (a) Hyperpolarized (left) membrane potentials (negative inside cell) promote PeT and quench fluorescence. Depolarization (positive inside cell) decreases PeT and increases fluorescence (right). Thus, the quantum yield of VF dyes is related to the local membrane potential. (b) General synthesis of VF dyes.

Table 1. Properties of VoltageFluor Dyes

compound	R ₁	R ₂	R ₃	R ₄	$E(D^+/D)$ (V) ^a	$E(A/A^-)$ (V) ^a	λ_{abs} (nm) ^b	λ_{em} (nm) ^b	ΔG_{00} (eV)	$\Delta G_{PeT} + w$ (eV)	% $\Delta F/F$ per 100 mV ^c	Φ_{Fl} ^b
VF2.1(diOMe).Cl	N(Me) ₂	OMe	OMe	Cl	0.033	-2.02	521	535	2.38	-0.325	20	0.26
VF2.1(OMe).Cl	N(Me) ₂	OMe	H	Cl	0.090	-2.02	522	536	2.38	-0.263	49	0.13
VF2.1(OMe).F	N(Me) ₂	OMe	H	F	0.090	-2.11	509	528	2.44	-0.243	44	0.05
VF2.1.Cl	N(Me) ₂	H	H	Cl	0.129	-2.02	522	536	2.38	-0.224	27	0.05
VF2.1.F	N(Me) ₂	H	H	F	0.129	-2.11	508	524	2.44	-0.209	30	0.10
VF2.1(diOMe).H	N(Me) ₂	OMe	OMe	H	0.033	-2.24	504	522	2.46	-0.186	30	0.24
VF2.1(OMe).H	N(Me)₂	OMe	H	H	0.090	-2.24	504	524	2.46	-0.130	48	0.04
VF2.1.H	N(Me) ₂	H	H	H	0.129	-2.24	507	528	2.45	-0.076	16	0.11
VF2.1(OMe).Me	N(Me) ₂	OMe	H	Me	0.090	-2.32	515	536	2.41	0.003	13	0.04
VF2.1.Me	N(Me) ₂	H	H	Me	0.129	-2.32	513	532	2.42	0.033	5	0.38
VF2.0.Cl	H	H	H	Cl	1.080 ^d	-2.02	521	538	2.38	0.722	0	0.50

^avs Ferrocene (Fc). ^b0.01% Triton X-100, 5 mM sodium phosphate, pH 9. ^cMeasured in voltage-clamped HEK cells. ^dOxidation potential of stilbene taken from ref 33.

fidelity.²³ VF2.1.Cl uses photoinduced electron transfer²⁴ (PeT) through a molecular wire as a platform to achieve fast, wavelength-independent voltage imaging in neurons. Voltage-Fluor dyes localize to the plasma membrane, where the free energy for PeT is affected by the local electric field. At hyperpolarized potentials, PeT is more favorable, and at depolarized potentials, PeT is less favorable. Considering that PeT and fluorescence are competing processes, the inverse is true for fluorescence, which can be monitored via traditional fluorescence imaging (Figure 1a). In this article, we show that the VoltageFluor platform offers a general chemical strategy for voltage imaging and that voltage sensitivity can be rationally increased through modulation of donor and acceptor electron affinities. We present the design and synthesis of a series of 10 new structurally related VoltageFluors, estimate the driving force for PeT (ΔG_{PeT}), and establish their utility for imaging transmembrane potential in cultured cells, dissociated mammalian neurons, and *ex vivo* leech ganglia. Finally, we demonstrate that VF2.1(OMe).H can report on both fast and slow voltage changes in acutely prepared rodent olfactory bulb slices.

RESULTS

Design, Synthesis, and Characterization of Voltage-Fluors. Our strategy for voltage sensing relies on proper orientation of a fluorophore–wire–donor construct into the

plasma membrane (Figure 1a). Sulfofluoresceins were an initial choice because the persistently ionized sulfonic acid ($pK_a < -2$) helps to prevent internalization of the sensor through the cellular membrane. Sulfofluoresceins also have demonstrated utility in two-photon fluorescence imaging, leaving open possibilities for *in vivo* applications.²⁵ The low attenuation values and ease of chemical synthesis²⁶ of phenylenevinylene (PPV) molecular wires made them an ideal choice for spacers between the donor and acceptor. Our previous study showed that two generations of PPV spacer provided excellent voltage sensitivity while maintaining sufficient loading and water solubility. Finally, nitrogenous donors are frequently used in PeT sensors^{27–30} and, in this case, offer the opportunity to tune the relative energetics of PeT by modulation of the electron richness of the aniline. Previous studies²³ show that although *N,N*-dibutylaniline-derived VF2.4.Cl had similar voltage sensitivities as those of *N,N*-dimethyl-substituted VF2.1.Cl the dimethyl analogue had a better signal-to-noise ratio, on account of increased uptake into cellular membranes; therefore, dimethyl analogues were used throughout this study.

We sought to explore the voltage sensitivity of VF2.1.Cl through substituent changes on both the fluorophore/acceptor and donor. The modular nature of the VF dye synthesis (Figure 1b) enabled rapid construction of several new derivatives listed in Table 1. Figure 1b outlines the synthesis of the VF family of dyes (full details are available in the Supporting Information).

All of the VF sensors were characterized spectroscopically in aqueous media (pH 9, 0.1% Triton X-100 to ensure complete solubility and deprotonated form of the xanthene phenol) and had absorption maxima ranging from 504 nm (VF2.1(OMe).H) to 522 nm (VF2.1Cl compounds) and emission profiles between 522 and 538 nm (Table 1). The substituent pattern on the xanthene chromophore determined the absorbance band, with unsubstituted sulfofluorescein displaying λ_{max} values centered around 506 nm, fluoro-substituted sulfofluorescein, at 508 nm, methyl, at 514 nm, and chloro, at 522 nm. Additionally, each VF compound exhibited a secondary absorbance band characteristic of a conjugated phenylenevinylene molecular wire, with λ_{max} values ranging from 392 to 410 nm (Figure 2b and Supporting Information

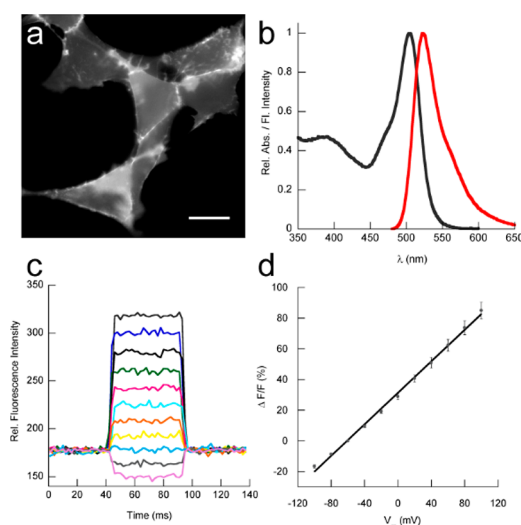


Figure 2. Characterization of VoltageFluor 2.1(OMe).H in HEK cells. (a) HEK cells stained with 200 nM VF2.1(OMe).H for 15 min at 37 °C. Scale bar is 20 μm . (b) Absorbance and emission profile of VF2.1(OMe).H at pH 9, 0.01% Triton X-100. (c) Fluorescence response of VF2.1(OMe).H in voltage-clamped cells from (a), plotted against time, during 50 ms steps from -60 mV to $+100$ mV followed by steps decreasing in potential by 20 mV increments to -100 mV. (d) Linearity of VF2.1(OMe).H response ($\Delta F/F$) vs final membrane potential in the physiologically relevant range (± 100 mV). Each data point represents three separate measurements. Error bars are \pm SEM for ≥ 3 separate experiments.

Figure 1). VF2.0.Cl had a secondary λ_{max} substantially blue-shifted from the other VF dyes (363 nm), owing to the lack of conjugation through the dimethylaniline. The quantum yields for the dyes ranged from 0.04 for VF2.1(OMe).Me to 0.50 for VF2.0.Cl (Table 1).

Fluorescence Response to Potential Changes. The voltage response of the dyes was established in whole-cell-patched, voltage-clamped HEK cells. Bath application of 200 nM VF dyes for 15 min at 37 °C resulted in cellular staining localized to the plasma membrane (Figures 2a and 3a; all images depict cells not under voltage-clamp, where V_m is close to -60 mV). Importantly, loading conducted at 37 °C did not result in significant internalization of the dye molecule. Furthermore, throughout the course of evaluation in HEK cells (45 to 60 min), we observed negligible dye internalization or loss of voltage sensitivity, as measured by the change in voltage sensitivity recorded from cells patched at the beginning

of a trial (approximately 5–15 min postloading) and at the end of a trial (approximately 30–60 min postloading).

The deviation in sensitivity is low ($<5\%$), and this is reflected in the small error bars in Figure 3b. This suggests that, under these conditions, the initial orientation of the dye within the membrane is established early during loading and very little inversion of the VoltageFluor occurs. We corroborated this finding by examining the cellular staining of VF dyes as a function of dye incubation time and found little change in the localization after loading VF2.1(OMe).H for either 10 or 85 min (Supporting Information Figure 2). Uniform orientation of the dyes is critical for obtaining voltage sensitivity because an equal distribution of chromophore-in and chromophore-out orientations would result in net zero voltage sensitivity (Figure 1a). Whole-cell voltage-clamped HEK cells were held at -60 mV and then stepped to hyper- and depolarizing potentials in 20 mV steps (range ± 100 mV, Figure 2c,d and Supporting Information Movie 1). After background subtraction, voltage sensitivities ranging from 4 to 49% $\Delta F/F$ per 100 mV were measured for the VF dyes, with VF2.1.Me being the least and VF2.1(OMe).Cl being the most sensitive. VF2.1(OMe).H displayed 48% $\Delta F/F$ per 100 mV (Supporting Information Figure 3 indicates an example of region of interest, ROI, selection for determining voltage sensitivity). Importantly, control compound VF2.0.Cl, which lacks an electron-rich aniline donor, shows no voltage sensitivity (Supporting Information Figure 4).

To further explore the linearity of the VF series, we applied a more extreme hyper- and depolarizing stepping paradigm to HEK cells loaded with VF dyes, assaying a range spanning ± 300 mV. Still larger steps proved too much of a strain on the cells and could not be reliably measured. At extremely hyperpolarizing potentials (large negative potential inside the cell), we hypothesized that PeT would be maximally activated and the VF dye would be at its dimmest state. Conversely, at larger depolarizing potential (large positive potential inside), PeT quenching would be entirely relieved, and the dye would be at its maximal brightness. Fluorescence responses were measured as before, and steps were provided in 30 mV increments to cover the range from ± 300 mV. The first-generation dye VF2.1.Cl, as well as VF2.1(diOMe).H, VF2.1(OMe).H, and VF2.1.F, fit within a range that encompassed, or nearly encompassed, the minimum and maximum, meaning that the 600 mV range of potentials spanned the energetics required to switch PeT completely on or off (Figure 3b). VF dyes bearing more electron-rich aniline donors (OMe, diOMe) and/or electron-poor fluorophores, such as VF2.1(diOMe).Cl, VF2.1(OMe).Cl, and VF2.1(OMe).F, showed fluorescence responses that generally comprised the lower bound of the sigmoidal curve at hyperpolarizing potentials, indicating that PeT processes dominate in this regime. Only at extremely depolarizing potentials (>100 mV) did significant voltage sensitivity manifest. A final grouping of dyes, including VF2.1.H, VF2.1(OMe).Me, and VF2.1.Me, displayed fluorescence responses confined to the asymptote achieved at extreme depolarizing potentials. In this regime, radiative pathways predominate, giving bright signals that can be quenched only upon extreme hyperpolarization of the cell membrane.

Estimation of ($\Delta G_{\text{PeT}} + w$). To gain a more quantitative understanding of the factors that contribute to voltage sensitivity, we measured the redox potentials of both the donors and acceptors within the VF framework. The oxidation and reduction potentials of dimethyl anilines and substituted

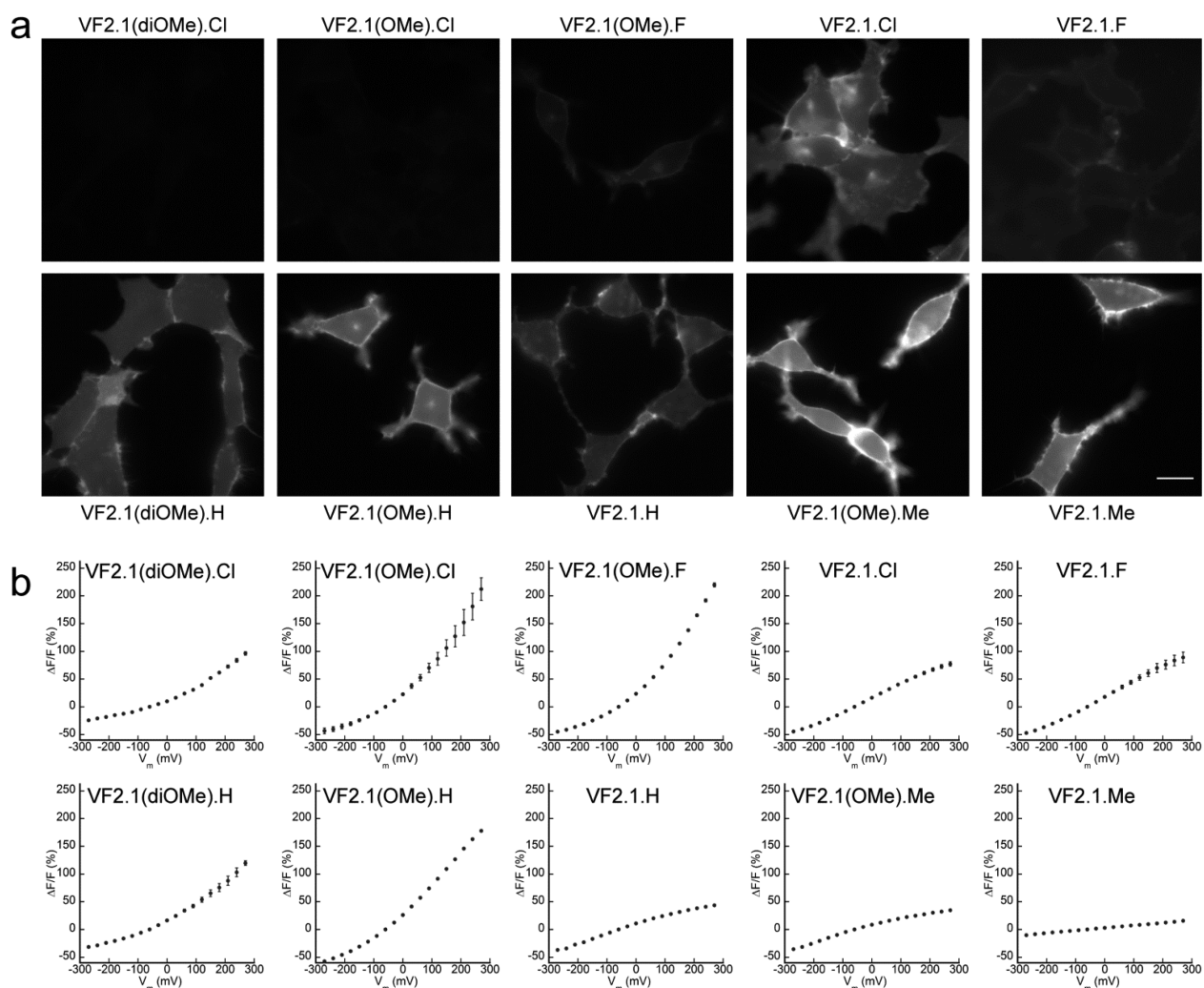


Figure 3. Staining and voltage sensitivity of VoltageFluor dyes in HEK cells. (a) Epifluorescence images of HEK cells incubated in HBSS buffer containing 200 nM of the indicated VoltageFluor dyes for 15 min at 37 °C. All acquisition and analysis parameters are identical to enable an estimation of the relative brightness of the dyes in a cellular context. Scale bar is 20 μm . Cells are not under voltage-clamp conditions. (b) Fluorescence response of representative VoltageFluor dyes vs membrane potential. Voltage-clamped HEK cells were held at -60 mV and then stepped to the indicated potential. The relative change in fluorescence ($\Delta F/F$) is plotted against the final membrane potential for VoltageFluor dyes loaded in HEK cells at a concentration of 200 nM. Error bars are \pm SEM for $n \geq 3$ for each dye.

sulfofluoresceins were measured via cyclic voltammetry. As expected, Cl-substituted sulfofluorescein was most readily reduced ($E(A/A^-) -2.02$ V vs ferrocene, Fc), followed by F-substituted sulfofluorescein (-2.10 V vs Fc). Unsubstituted sulfofluorescein was 130 mV more difficult to reduce (-2.24 V vs Fc), and Me-substituted sulfofluorescein was the most difficult to reduce (-2.32 V vs Fc) (Supporting Information Figure 5). Measuring oxidation potentials of the donors proved to be more challenging, as the resulting radical cations undergo further oxidation and reaction to form benzidine species,³¹ limiting our ability to report oxidation potentials of the pure dimethylaniline species. We instead measured the oxidation potential of synthetic intermediates **4**, which, on account of substitution *para* to the dimethylamino group, restricted formation of confounding dimeric species. Oxidation of the phenylenevinylene dimethylanilines was still fairly reactive, giving irreversible voltammograms, but provided more reliable initial oxidation measurements (Supporting Information Figure 5). The unsubstituted donor measured at the initial oxidation peak was the least readily oxidized ($E(D/D^+) +0.129$ V vs Fc). A single methoxy substitution *ortho* to the dimethylamino

group gave an oxidation potential of 0.090 V vs Fc, whereas 2,5-dimethoxy aniline was the most readily oxidized at 0.033 V vs Fc. With these values in hand, we could estimate the driving force for PeT through the use of the Rehm–Weller equation,³² $\Delta G_{\text{PeT}} = \Delta E_{\text{ox}} - \Delta E_{\text{red}} - \Delta E_{0,0} - w$, where ΔE_{ox} is the oxidation potential of the donor, ΔE_{red} is the reduction potential of the acceptor/fluorophore, $\Delta E_{0,0}$ is the energy required to excite the chromophore into the first electronically excited state, and w is a work term representing the energy required to separate two charges. Due to the minor structural differences between the VF compounds, w remains relatively constant across the VF series, although its absolute magnitude remains difficult to estimate with precision. The $(\Delta G_{\text{PeT}} + w)$ values are summarized in Table 1.

VF dyes bearing electron-withdrawing groups (Cl, F) on the fluorophore and electron-donating groups (OMe, diOMe) on the donor had the most negative $(\Delta G_{\text{PeT}} + w)$ values, whereas VF dyes with electron-donating (H, Me) fluorophores and unsubstituted dimethylanilines had the highest $(\Delta G_{\text{PeT}} + w)$ values. The experimentally estimated $(\Delta G_{\text{PeT}} + w)$ values correlates well with the fluorescence response of the VF dyes at

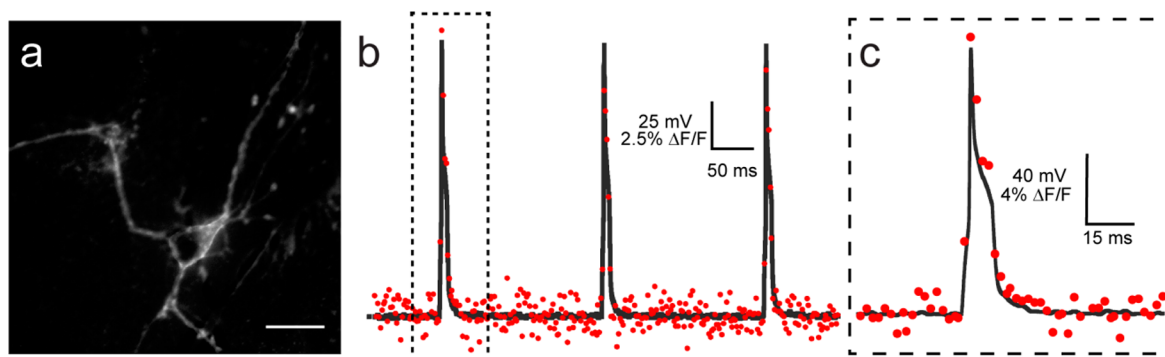


Figure 4. Application of VF2.1(OMe).H to sensing action potentials in cultured neurons. (a) Epifluorescence image of cultured rat hippocampal/cortical neurons stained with 200 nM VF2.1(OMe).H for 15 min at 37 °C. Scale bar is 20 μm . (b) Dual optical and electrophysiological recordings of evoked action potentials in cultured neurons. (c) Expanded time scale of the first stimulation in (b).

extreme potentials. For the three dyes with ($\Delta G_{\text{peT}} + w$) values lower than -0.23 eV, VF2.1(diOMe).Cl, VF2.1(OMe).Cl, and VF2.1(OMe).F, voltage sensitivity was moderate to high (20–49% $\Delta F/F$ per 100 mV) in the physiologically relevant window of ± 100 mV (Table 1 and Figure 3b). However, the response was not linear, and significant quenching is observed at hyperpolarizing/neutral potentials. Only upon achieving more extreme depolarizing potentials do these dyes unquench to give significant fluorescence responses to changing membrane potentials (Figure 3b). Conversely, for the three VF dyes with ($\Delta G_{\text{peT}} + w$) greater than -0.08 eV, sufficient driving force is not available to quench fluorescence, so radiative pathways dominate VF2.1.H, VF2.1(OMe).Me, and VF2.1.Me (Figure 3b).

This results in low voltage sensitivity (5–16% $\Delta F/F$ per 100 mV) in the physiological range that becomes larger only upon increased hyperpolarization. Finally, the four VF dyes with intermediate ($\Delta G_{\text{peT}} + w$) values, ranging from -0.13 to -0.22 eV, show the most linear responses to membrane potential changes within the physiologically relevant range of ± 100 mV (Figure 3b), with moderate (27%) to high (48%) voltage sensitivity (Table 1). These dyes include VF2.1.Cl, VF2.1.F, VF2.1(diOMe).H, and VF2.1(OMe).H. These data suggest that a threshold of ($\Delta G_{\text{peT}} + w$) values less than -0.08 eV, but no lower than -0.27 eV, are required to achieve voltage sensitivity greater than 20% $\Delta F/F$ per 100 mV. Two dyes that meet this criteria, VF2.1(OMe).Cl and VF2.1(OMe).H, show high voltage sensitivity, at 49 and 48% $\Delta F/F$ per 100 mV, a $>80\%$ improvement over the initial VF2.1.Cl compound. Although the absolute sensitivity of VF2.1(OMe).Cl is marginally greater than VF2.1(OMe).H, the more negative ($\Delta G_{\text{peT}} + w$), which results in more quenching at physiological membrane potential, makes VF2.1(OMe).H more suitable for investigations of membrane potential fluctuations at or near -60 mV (nominal resting membrane potential for many neurons). Additionally, the brighter staining of HEK cells with VF2.1(OMe).H over VF2.1(OMe).Cl made it the optimal probe for subsequent biological applications.

Characterization of VF2.1(OMe).H in Neurons. First, we applied VF2.1(OMe).H to cultured cortical neurons (Figure 4). Bath application of the dye extensively stained neuronal cell membranes, as determined by epifluorescence microscopy (Figure 4a). Confocal imaging of VF2.1(OMe).H-stained neurons established localization to the cellular membrane with very little visible internalization (Supporting Information Figure 6). These experiments also show little internalization

even with an extended loading time of 2 h (Supporting Information Figure 6). VF2.1(OMe).H readily detected action potentials in single trials (Figure 4b,c and Supporting Information Movie 2) with a signal-to-noise ratio of 28:1, a near 2-fold improvement over VF2.1.Cl.²³ The inherently fast nature by which VF dyes sense changes in membrane potential ($\tau_{\text{on/off}} < 150 \mu\text{s}$)²³ offers superior fidelity in reproducing electrical signals compared to protein-based sensors with longer response times, for example, ArcLight Q239 ($\tau_{\text{on/off}} = 10\text{--}50$ ms).¹⁸

One of the promises of voltage imaging is the ability to spatially reconstruct patterns of activity within a functional network. For this purpose, the medicinal leech has proven to be an important model system for understanding circuit dynamics because it not only contains several hundred functionally connected neurons but also provides ready access to both electrophysiological and voltage-sensitive optical recording. Small molecule indicators have a distinct advantage over protein-based indicators because of the difficulty of transfecting adult leech neurons.³⁴ We prepared desheathed midbody ganglia from *Hirudo medicinalis* stained with VF2.1(OMe).H (200 nM, 20 min). Following treatment with VF2.1(OMe).H, cellular membranes in the ganglia showed strong fluorescence characteristic of VF dyes (Figure 5a). Using paired electrode recording (20–40 $M\Omega$) in conjunction with fluorescence imaging, we monitored fluorescence as a function of membrane potential. Spontaneously firing action potentials from the Retzius cell were clearly distinguished optically (Figure 5b, red trace), and the time course matched that of the intracellular electrode (Figure 5b, black trace). VF2.1(OMe).H detects not only supra-threshold spikes but also slower depolarization and repolarizations following action potential. These repolarizations were not observed in the rat optical or electrophysiological traces due to a stimulus artifact that bled slightly into the repolarization phase of the action potential. In both cases (rat and leech), the optical trace clearly follows the electrophysiology, establishing the fidelity of the VF dyes for tracking real membrane potential changes. The action potentials in the leech optical recording appear to be truncated due to undersampling in the fluorescence channel (acquisition speed is 50 Hz). The fractional change in fluorescence is approximately 3-fold larger than with VF2.1.Cl,²³ consistent with the improvement (approximately 2-fold) observed in HEK cells.

Next, we assessed the ability of the dye to detect voltage changes in brain slices, a more challenging endeavor

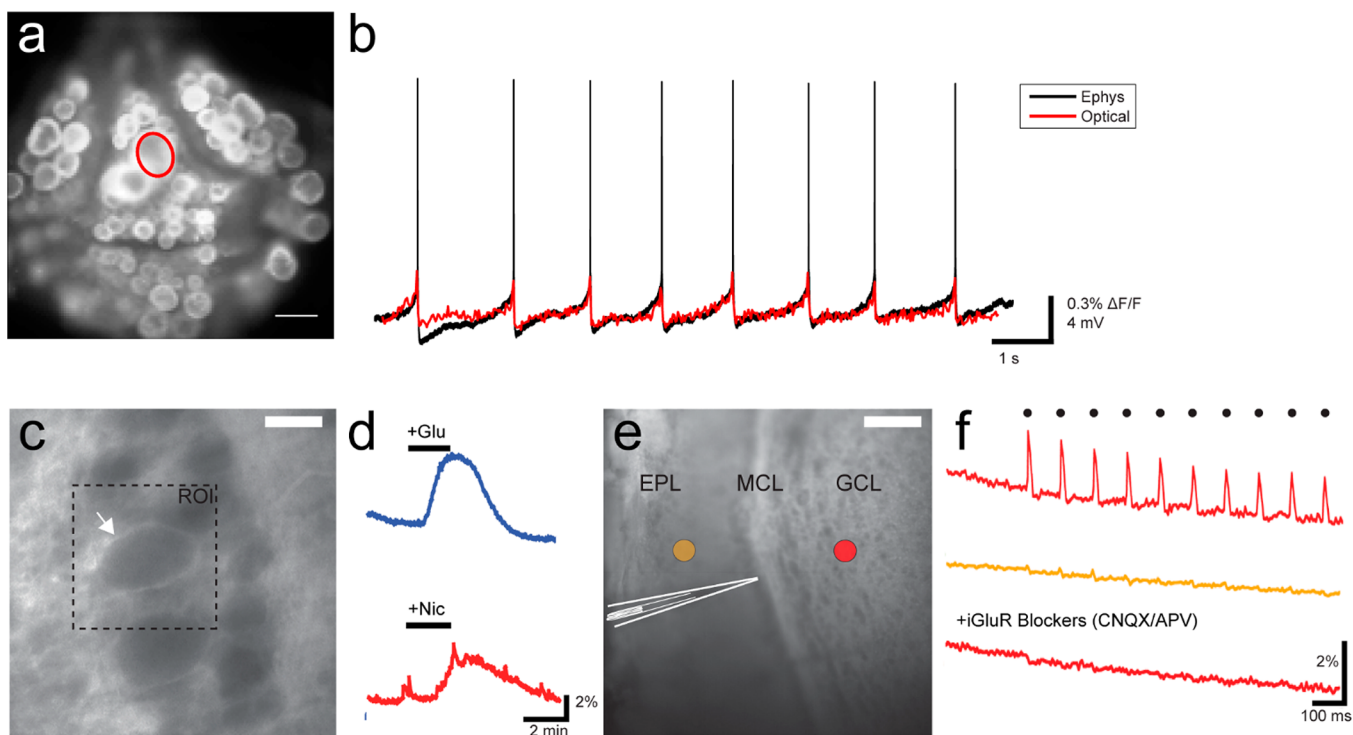


Figure 5. Applications of VF2.1(OMe).H. (a) Epifluorescence image of *H. medicinalis* midbody ganglia stained with VF2.1(OMe).H. Scale bar is 50 μm . (b) Optical (red) and electrophysiological (black) recording of spontaneous activity in the leech ganglia from regions of interest (ROI) indicated in (a). The calibration bar is 0.3% $\Delta F/F$, 4 mV, and 1 s. (c) Epifluorescence image of a sagittal mouse olfactory bulb (OB) slice loaded with VF2.1(OMe).H (500 nM). The dotted square represents the ROI used for quantification. The white arrow points to the plasma membrane of a mitral cell (MC) loaded with VF dye. The scale bar is 10 μm . (d) Optical recordings (0.5 Hz acquisition) showing the fluorescence response of VF2.1(OMe).H in the cell from (c) to glutamate (blue trace, +Glu, 100 μM , 1.5 min) and nicotine (red trace, +Nic, 30 μM , 1.5 min). The calibration bar is 2% $\Delta F/F$ and 2 min. (e) Epifluorescence wide-field view of another olfactory bulb slice loaded with VF2.1(OMe).H. A patch electrode was used to electrically stimulate in the vicinity of the MC layer (MCL). The top calibration bar is 50 μm . Orange and red circles indicate ROIs used for analysis in (f). (f) Optical recordings (200 Hz acquisition) in the external plexiform layer (EPL, orange) or granule cell layer (GCL, red). The timing of the stimulus pulse is indicated by black dots (10 ms, 10 Hz). The stimulus produces a voltage change in the GCL (upper red trace) but not in the external plexiform layer (EPL, middle orange trace). The responses in the GCL are abolished in the presence of ionotropic glutamate receptors (iGluR) blockers (APV, 100 μM ; CNQX, 10 μM ; bottom red trace). The calibration bar is 2% $\Delta F/F$ and 100 ms.

considering the complexity, scale, and diversity of the preparation. Efforts to visualize voltage changes in slice are hampered by small fractional changes in fluorescence. State-of-the-art indicators all have significant shortcomings in this context. For example, the low brightness of QuasAr requires intense laser power to achieve sensing, limiting the observable field to $\sim 200 \mu\text{m}^2$ before tissue heating becomes a concern.²² Small molecule voltage-sensitive dyes have inherent limitations as well, particularly with indiscriminate staining of all plasma membranes. Increasing the voltage sensitivity of indicators can partially ameliorate this obstacle, so we were hopeful that the improved sensitivity of VF2.1(OMe).H would allow us to measure membrane potential changes optically in a brain slice.

We turned to the olfactory bulb (OB) of mice because it contains a well-characterized synaptic connectivity that has largely been explored through traditional electrophysiological means³⁵ or by optical imaging through absorbance techniques.³⁶ Within the OB, sensory input excites principal neurons, the mitral and tufted cells (MCs). Activation of MCs excites, via ionotropic glutamate receptors, surrounding local inhibitory neurons, or granule cells (GCs).³⁷ Staining of OB slices with VF2.1(OMe).H (500 nM, 20 min incubation) resulted in strong fluorescence signals from the cell membranes of OB neurons, in particular, the large MCs (Figure 5c, white arrow). Activation of MCs by bath application of glutamate gives a large

increase in fluorescence intensity, lasting several minutes (optical recording rate = 0.5 Hz) and consistent with activation of the MCs (Figure 5d, "G", 100 μM , 2 min; $4.13 \pm 0.40\%$, $n = 6$, $p < 0.01$). Additionally, in agreement with previous findings,³⁵ application of the acetylcholine receptor agonist, nicotine (Figure 5d, "N", 30 μM , 2 min), also depolarized MCs ($\Delta F/F$, $3.02 \pm 0.27\%$, $n = 6$, $p < 0.01$). Next, we conducted electrical stimulations (10 ms pulses, 10 Hz) in the vicinity of the MC layer (MCL) to synaptically activate GCs while optically recording (200 Hz frame rate) from this cell layer (GCL). Focal electrical stimulation revealed a fast, robust increase in fluorescence in the GCL (Figure 5e,f, red circle and red upper trace, $\Delta F/F$ $1.91 \pm 0.23\%$, $n = 5$, $p < 0.01$) owing to activation of GCs by glutamate released from MCs. Importantly, this excitation did not elicit a response in the external plexiform layer (EPL, Figure 5e,f, orange circle and trace), demonstrating that VF2.1(OMe).H efficiently tracks synaptic transmission from the MCL to the GCL and that this response does not result from a nonselective depolarization of the stimulated region. Accordingly, the excitation was sensitive to ionotropic glutamate receptor (iGluR) blockade by APV and CNQX (Figure 5f, red lower trace, 100 and 10 μM ; $\Delta F/F$, $0.07 \pm 0.15\%$, $n = 5$, $p < 0.01$). When the same experiments were conducted with VF2.1.Cl in order to compare its performance vs VF2.1(OMe).H, the optical response to identical stimulation

was substantially larger for VF2.1(OMe).H, consistent with results in HEK cells, rat neurons, and leech ganglia. The response from VF2.1(OMe).H was 2-fold larger than VF2.1.Cl for electrical stimulation and 3- to 4-fold larger under stimulation with glutamate or nicotine, respectively ($p < 0.0015$ in all cases, t -test, $n = 6$; Supporting Information Figure 7). These experiments and direct comparisons demonstrate the utility of the VF dyes, and especially VF2.1(OMe).H, for conducting both fast and slow *in vitro* slice network physiology.

DISCUSSION

Voltage imaging with small molecules has been limited to staining of single cells in a brain slice³⁸ or to measurement of optical “field potentials” that report population changes and require spike-timed averaging.³⁹ One problem has been the lack of fast, sensitive, and nondisruptive probes to report on membrane potential changes. To address this concern, we here report the design, synthesis, and application of a new family of voltage-sensitive dyes, VoltageFluors (VFs), that make use of photoinduced electron transfer from an electron-rich aniline through a conjugated phenylenevinylene molecular wire to a xanthene chromophore for fast, sensitive voltage sensing in a variety of neuronal contexts. The VF family of dyes displays visible excitation and emission profiles that enable optical voltage recording at peak excitation and emission wavelengths, large linear responses to changes in membrane potential, negligible capacitance loading of membranes, and fast turn-on optical responses capable of resolving action potentials and subthreshold membrane potential dynamics in neurons.

As a chemical platform, the VF dyes offer a tunable approach to voltage sensing, in which alteration of the electron affinities results in modulation of the voltage sensitivity of the dye. This study demonstrates, for the first time, that modulation of ΔG_{PeT} alters the voltage sensitivity of VF dyes and establishes unequivocally the requirement of an electron-rich donor for voltage sensing, as indicated by the lack of voltage response from VF2.0.Cl. Analysis of the relative driving force for electron transfer derived from experimentally determined oxidation/reduction potentials suggests that the range of -0.08 to -0.27 V yields sensors with high voltage sensitivity and linearity within a physiologically relevant window of ± 100 mV. The most sensitive of the VF dyes, VF2.1(OMe).Cl and VF2.1(OMe).H, have voltage sensitivities of 49 and 48% $\Delta F/F$ per 100 mV, respectively, and compare favorably to other fast voltage dyes that function via an electrochromic sensing mechanism and have typical voltage sensitivities ranging from 10 to 28% $\Delta F/F$ per 100 mV.^{38,40} Although high voltage sensitivities can be achieved with electrochromic dyes by excitation at the far-red edge of the excitation spectrum and collection with a similarly narrow emission filter, this requires off-peak excitation, the use of potentially phototoxic high-intensity illumination, and sampling of only a small fraction of emitted, voltage-sensitive photons.⁴¹ For voltage imaging, which is inherently photon-limited due to the fast sampling nature (0.5–2 kHz range) of the experiment, sacrificing the majority of excitation and emission photons can be problematic, making approaches such as VF dyes, which use all excitation and emission photons for sensing, ideally suited for voltage imaging. Due to its improved linear response to membrane potential change, we used VF2.1(OMe).H to monitor action potentials in cultured neurons with enhanced SNR over previous VF dyes (28:1 vs 16:1). We also demonstrated the enhanced utility of VF2.1(OMe).H in leech

ganglia for monitoring spontaneous activity with a 3-fold improvement of SNR compared to VF2.1.Cl. Finally, applications in brain slices show that VF2.1(OMe).H can report on both slow and fast network physiology in a complex neuronal environment. The performance of VF2.1(OMe).H in these preparations are summarized in Table 2.

Table 2. VF2.1(OMe).H Performance in Biological Samples

sample	$\Delta F/F$	SNR
HEK cells	48% ^a	38:1
rat neurons	10% ^a	28:1
leech neurons	2–4% ^{a,b}	17:1
olfactory bulb slice	2% ^c	17:1

^aPer 100 mV change, calibrated by simultaneous electrophysiological measurement. ^bNo background subtraction. Images sampled at 50 Hz. ^cUncalibrated; no background subtraction.

The optimal voltage probe remains elusive. The best voltage-sensitive proteins, QuasAr1,²² ASAP1,²⁰ and ArcLight Q239,¹⁸ have issues with brightness, sensitivity, and speed, respectively. In addition, the turn-off response of ASAP1 and ArcLight Q239 to depolarization decreases sensitivity. These issues have been addressed by VF dyes. Current VF dyes represent a significant advance in sensitivity over previous VF dye incarnations, although much work remains. First, because VF dyes have no genetically encoded component yet, promiscuous staining of nonexcitable cells in heterogeneous samples severely decreases the apparent voltage sensitivity by raising the overall background fluorescence. This trend is apparent in the decreased voltage sensitivity and SNR upon going from HEK cells to brains slices (Table 2). Genetic targeting of VF dyes in a two-component system would enable analysis of genetically defined cells and improve the signal-to-noise ratio. Second, VF2.1(OMe).H, described here, shows a greater than 100% $\Delta F/F$ per 100 mV at extremely depolarized potentials, indicating that greater sensitivities can be achieved. Third, longer wavelengths would be beneficial for thick samples and multiplex imaging with currently available probes. The generality of the VoltageFluor PeT platform predicts the chemical tractability of these efforts, which are ongoing in our laboratories.

ASSOCIATED CONTENT

Supporting Information

Experimental details including synthesis and characterization of all VoltageFluor dyes and precursors; cyclic voltammetry, electrophysiology, and cell imaging data. This material is available free of charge via the Internet at <http://pubs.acs.org>.

AUTHOR INFORMATION

Corresponding Authors

*(E.W.M.) evanwmiller@berkeley.edu

*(R.Y.T.) rtsien@ucsd.edu

Present Address

[†](E.W.M.) Departments of Chemistry and Molecular & Cell Biology, UC Berkeley, Berkeley, California 94720, United States.

Author Contributions

◆C.R.W. and E.W.M. contributed equally to this work.

Notes

The authors declare the following competing financial interest(s): E.W.M. and R.Y.T. are listed as inventors on a

patent describing voltage-sensitive dyes owned by the University of California and licensed to Life Technologies.

■ ACKNOWLEDGMENTS

This work was supported by the Howard Hughes Medical Institute, NIH R37NS027177 to R.Y.T., a Pathways to Independence Award to E.W.M. (K99/R00NS078561), NIH MH43396 and NSF IOB-0523959 to W.B.K., NIH Training Grants EB009380 and MH020002 to E.P.F., NSF CHE-1145893 and AFOSR FA 9550-13-1-0020 to C.P.K. and G.C., and NIH DC009817 to R.C.A.

■ REFERENCES

- (1) Scanziani, M.; Hausser, M. *Nature* **2009**, *461*, 930.
- (2) Salzberg, B. M.; Davila, H. V.; Cohen, L. B. *Nature* **1973**, *246*, 508.
- (3) Johnson, L. V.; Walsh, M. L.; Chen, L. B. *Proc. Natl. Acad. Sci. U.S.A.* **1980**, *77*, 990.
- (4) Grinvald, A.; Fine, A.; Farber, I. C.; Hildesheim, R. *Biophys. J.* **1983**, *42*, 195.
- (5) Fluhler, E.; Burnham, V. G.; Loew, L. M. *Biochemistry* **1985**, *24*, 5749.
- (6) Fromherz, P.; Hubener, G.; Kuhn, B.; Hinner, M. J. *Eur. Biophys. J.* **2008**, *37*, 509.
- (7) Gonzalez, J. E.; Tsien, R. Y. *Biophys. J.* **1995**, *69*, 1272.
- (8) Chanda, B.; Blunck, R.; Faria, L. C.; Schweizer, F. E.; Mody, I.; Bezanilla, F. *Nat. Neurosci.* **2005**, *8*, 1619.
- (9) Bradley, J.; Luo, R.; Otis, T. S.; DiGregorio, D. A. *J. Neurosci.* **2009**, *29*, 9197.
- (10) Sjulson, L.; Miesenbock, G. *J. Neurosci.* **2008**, *28*, 5582.
- (11) Millard, A. C.; Jin, L.; Wei, M. D.; Wuskell, J. P.; Lewis, A.; Loew, L. M. *Biophys. J.* **2004**, *86*, 1169.
- (12) Reeve, J. E.; Corbett, A. D.; Boczarow, I.; Kaluza, W.; Barford, W.; Bayley, H.; Wilson, T.; Anderson, H. L. *Angew. Chem., Int. Ed.* **2013**, *52*, 9044.
- (13) Park, K.; Deutsch, Z.; Li, J. J.; Oron, D.; Weiss, S. *ACS Nano* **2012**, *6*, 10013.
- (14) Marshall, J. D.; Schnitzer, M. J. *ACS Nano* **2013**, *7*, 4601.
- (15) Siegel, M. S.; Isacoff, E. Y. *Neuron* **1997**, *19*, 735.
- (16) Tsutsui, H.; Karasawa, S.; Okamura, Y.; Miyawaki, A. *Nat. Methods* **2008**, *5*, 683.
- (17) Barnett, L.; Platasa, J.; Popovic, M.; Pieribone, V. A.; Hughes, T. *PLoS One* **2012**, *7*, e43454.
- (18) Jin, L.; Han, Z.; Platasa, J.; Wooldorton, J. R.; Cohen, L. B.; Pieribone, V. A. *Neuron* **2012**, *75*, 779.
- (19) Akemann, W.; Sasaki, M.; Mutoh, H.; Imamura, T.; Honkura, N.; Knopfel, T. *Sci. Rep.* **2013**, *3*, 2231.
- (20) St-Pierre, F.; Marshall, J. D.; Yang, Y.; Gong, Y.; Schnitzer, M. J.; Lin, M. Z. *Nat. Neurosci.* **2014**, *17*, 884.
- (21) Kralj, J. M.; Douglass, A. D.; Hochbaum, D. R.; Maclaurin, D.; Cohen, A. E. *Nat. Methods* **2012**, *9*, 90.
- (22) Hochbaum, D. R.; Zhao, Y.; Farhi, S. L.; Klapoetke, N.; Werley, C. A.; Kapoor, V.; Zou, P.; Kralj, J. M.; Maclaurin, D.; Smedemark-Margulies, N.; Saulnier, J. L.; Boulting, G. L.; Straub, C.; Cho, Y. K.; Melkonian, M.; Wong, G. K.; Harrison, D. J.; Murthy, V. N.; Sabatini, B. L.; Boyden, E. S.; Campbell, R. E.; Cohen, A. E. *Nat. Methods* **2014**, *11*, 825.
- (23) Miller, E. W.; Lin, J. Y.; Frady, E. P.; Steinbach, P. A.; Kristan, W. B.; Tsien, R. Y. *Proc. Natl. Acad. Sci. U.S.A.* **2012**, *109*, 2114.
- (24) Li, L.-s. *Nano Lett.* **2007**, *7*, 2981.
- (25) Tanner, G. A.; Sandoval, R. M.; Dunn, K. W. *Am. J. Physiol.: Renal Physiol.* **2004**, *286*, F152.
- (26) Davis, W. B.; Svec, W. A.; Ratner, M. A.; Wasielewski, M. R. *Nature* **1998**, *396*, 60.
- (27) Minta, A.; Kao, J. P.; Tsien, R. Y. *J. Biol. Chem.* **1989**, *264*, 8171.
- (28) Kojima, H.; Nakatsubo, N.; Kikuchi, K.; Kawahara, S.; Kirino, Y.; Nagoshi, H.; Hirata, Y.; Nagano, T. *Anal. Chem.* **1998**, *70*, 2446.
- (29) He, Q.; Miller, E. W.; Wong, A. P.; Chang, C. J. *J. Am. Chem. Soc.* **2006**, *128*, 9316.
- (30) Zheng, S.; Lynch, P. L. M.; Rice, T. E.; Moody, T. S.; Gunaratne, H. Q. N.; de Silva, A. P. *Photochem. Photobiol. Sci.* **2012**, *11*, 1675.
- (31) Larumbe, D.; Gallardo, I.; Andrieux, C. P. *J. Electroanal. Chem. Interfacial Electrochem.* **1991**, *304*, 241.
- (32) Rehm, D.; Weller, A. *Israel J. Chem.* **1970**, *8*, 259.
- (33) Adams, B. K.; Cherry, W. R. *J. Am. Chem. Soc.* **1981**, *103*, 6904.
- (34) Baker, M. W.; Macagno, E. R. *J. Neurosci. Methods* **2006**, *156*, 145.
- (35) Smith, R. S.; Araneda, R. C. *J. Neurophysiol.* **2010**, *104*, 2963.
- (36) Keller, A.; Yagodin, S.; Aroniadou-Anderjaska, V.; Zimmer, L. A.; Ennis, M.; Sheppard, N. F., Jr.; Shipley, M. T. *J. Neurosci.* **1998**, *18*, 2602.
- (37) Shipley, M. T.; Ennis, M. *J. Neurobiol.* **1996**, *30*, 123.
- (38) Yan, P.; Acker, C. D.; Zhou, W. L.; Lee, P.; Bollensdorff, C.; Negrean, A.; Lotti, J.; Sacconi, L.; Antic, S. D.; Kohl, P.; Mansvelter, H. D.; Pavone, F. S.; Loew, L. M. *Proc. Natl. Acad. Sci. U.S.A.* **2012**, *109*, 20443.
- (39) Refojo, D.; Schweizer, M.; Kuehne, C.; Ehrenberg, S.; Thoeniger, C.; Vogl, A. M.; Dedic, N.; Schumacher, M.; von Wolff, G.; Avrabos, C.; Touma, C.; Engblom, D.; Schutz, G.; Nave, K. A.; Eder, M.; Wotjak, C. T.; Sillaber, I.; Holsboer, F.; Wurst, W.; Deussing, J. M. *Science* **2011**, *333*, 1903.
- (40) Kuhn, B.; Fromherz, P. *J. Phys. Chem. B* **2003**, *107*, 7903.
- (41) Kuhn, B.; Fromherz, P.; Denk, W. *Biophys. J.* **2004**, *87*, 631.